

minimum energy path turns the corner in the  $r_{AB}$ ,  $r_{BC}$  coordinate system than it is in either asymptotic region. In the corner turning region, the reaction coordinate is changing from an A-HB motion to an AH-B one, and the bond stretching motion is changing from a high-frequency A-H hydride vibration to a low-frequency A-H-B symmetric or nearly symmetric stretch and then to a high-frequency H-B hydride vibration. This corresponds to a wide, high-entropy reaction channel in the corner-turning region, and it means that a lower entropy, higher free energy bottleneck is likely to be found elsewhere. The effect can also be described in a more dynamic language. When A and B are heavy, the time scale for A-HB and AH-B motions is slower than that for hydride vibrations or, in the corner-turning region, for rapid transfer of H back and forth between the heavy atoms. This transfer back and forth has been observed in various trajectory calculations.<sup>22</sup> It corresponds to successive recrossings of a symmetric or nearly symmetric dividing surface and means that the fundamental recrossing assumption<sup>23</sup> of classical transition state theory is not well satisfied for such a dividing surface. Thus it is unlikely that such a dividing surface provides the variationally best transition state for this mass combination. Although the effect is quantitatively largest for symmetric H-atom transfers, the present paper shows that this kind of skew angle effect also largely explains the quantitative differences of conventional transition state theory from canonical variational theory for a more general class of reactions, e.g., for Cl + CCl and Cl + BF.

### Concluding Remarks

The present study of 37 reactions involving the transfer of atoms other than hydrogen provides a survey of the effects of varying the location of the dividing surface on the thermal rate constants calculated by generalized transition state theory. Thermal rate constants are computed using conventional transition state theory and canonical variational theory, in both cases with quantized energy levels including anharmonicity. Comparison of the results indicates that there may be large

effects of varying the location of the generalized transition state dividing surfaces for certain kinds of reactions. The largest effects in the present study are generally associated with the looser complexes. In these cases the dominant factor is the tightening of the bending motion as the dividing surface is varied to a more symmetric location. For systems with endoergicities greater than 30 kcal/mol, the average ratio<sup>24</sup> of the conventional transition state theory rate constant to the canonical variational theory one increases from 1.25 at 200 K to 2.53 at 4000 K.

### References and Notes

- (1) Garrett, B. C.; Truhlar, D. G. *J. Phys. Chem.* **1979**, *83*, 1052.
- (2) Garrett, B. C.; Truhlar, D. G. *J. Phys. Chem.* **1979**, *83*, 1079. For a review see: Truhlar, D. G. *Ibid.* **1979**, *83*, 188.
- (3) Garrett, B. C.; Truhlar, D. G. *J. Am. Chem. Soc.*, **1979**, *101*, 4534.
- (4) Garrett, B. C.; Truhlar, D. G. *J. Phys. Chem.* **1979**, *83*, 200.
- (5) Johnston, H. S.; Parr, C. A. *J. Am. Chem. Soc.* **1963**, *85*, 2444.
- (6) Johnston, H. S. "Gas Phase Reaction Rate Theory", Ronald Press: New York, 1966.
- (7) Mayer, S. W.; Schieler, L.; Johnston, H. S. "Eleventh Symposium (International) on Combustion", Combustion Institute: Pittsburgh, 1967; p 837.
- (8) Mayer, S. W.; Schieler, L.; Johnston, H. S. *J. Chem. Phys.* **1966**, *45*, 385.
- (9) Mayer, S. W.; Schieler, L. *J. Phys. Chem.* **1968**, *72*, 236.
- (10) Mayer, S. W.; Schieler, L. *J. Phys. Chem.* **1968**, *72*, 2628.
- (11) Rosen, B. "Spectroscopic Data Relative to Diatomic Molecules", Pergamon Press: Elmsford, N.Y., 1970.
- (12) Stull, D. R., Ed. "JANAF Thermochemical Tables", Dow Chemical Co.: Midland, Mich., 1971.
- (13) Herzberg, G. "Spectra of Diatomic Molecules", Van Nostrand: Princeton, N.J., 1950.
- (14) Pauling, L. "The Nature of the Chemical Bond", Cornell University Press: Ithaca, N.Y., 1960.
- (15) Garrett, B. C.; Truhlar, D. G. *J. Phys. Chem.*, **1979**, *83*, 1915.
- (16) Hirschfelder, J. O.; Curtiss, C. F.; Bird, R. B. "Molecular Theory of Gases and Liquids", Wiley: New York, 1964.
- (17) See, e.g., Previtali, C. M.; Scaiano, J. S. *J. Chem. Soc. B* **1971**, 2317.
- (18) Wigner, E. P. *Z. Phys. Chem., Abt. B* **1932**, *19*, 203.
- (19) Truhlar, D. G. *J. Chem. Phys.* **1972**, *56*, 3189. Erratum: **1974**, *61*, 440. Muckerman, J. T.; Newton, M. D. *J. Chem. Phys.* **1972**, *56*, 3191.
- (20) Hammond, G. S. *J. Am. Chem. Soc.* **1955**, *77*, 334.
- (21) Miller, W. H. *J. Chem. Phys.* **1976**, *65*, 2216.
- (22) See, e.g., Pattengill, M. D.; Polanyi, J. C. *Chem. Phys.* **1974**, *3*, 1.
- (23) Wigner, E. *Trans. Faraday Soc.* **1938**, *34*, 29. Miller, W. H. *J. Chem. Phys.* **1975**, *62*, 1899.
- (24) This ratio is identical for the reverse exoergic reactions.

## Doubly Bridged Species as Transition States or Intermediates in Transition Metal Redox Reactions

Jeremy K. Burdett

Contribution from the Department of Chemistry, The University of Chicago, Chicago, Illinois 60637. Received March 27, 1979

**Abstract:** The molecular orbital structures of symmetrically doubly bridged  $M_2X_{10}$  complexes ( $D_{2h}$ ) are examined to determine for which d electron configurations this geometry is a stable intermediate or an unstable transition state. For almost all electronic configurations the structure is predicted to be stable but with a low-energy  $b_{3g}$  distortion (leading eventually to two five-coordinate units). For the remaining few configurations the structure is predicted to be unstable with decay via the  $b_{1u}$  route (leading to six- and four-coordinate units). The predictions correlate favorably with observed crystal structures. Kinetically this second result leads overall to two-ligand transfer as experimentally observed in several cases. It is pointed out that experimental detection of the one-ligand transfer route by product analysis does not exclude a doubly bridged intermediate which decays by the  $b_{3g}$  route.

### Introduction

We have recently used simple molecular orbital ideas to view<sup>1</sup> in a fresh light the intimate mechanism of redox reactions between transition-metal ions in solution.<sup>2-4</sup> For inner-sphere

reactions we found that whether the symmetrically bridged species **1** is an intermediate or transition state is simply determined by the electron configuration of the reacting ions  $M_1$  and  $M_2$ . In this paper we examine the role of the doubly bridged species **2**. Experimental evidence for double bridging

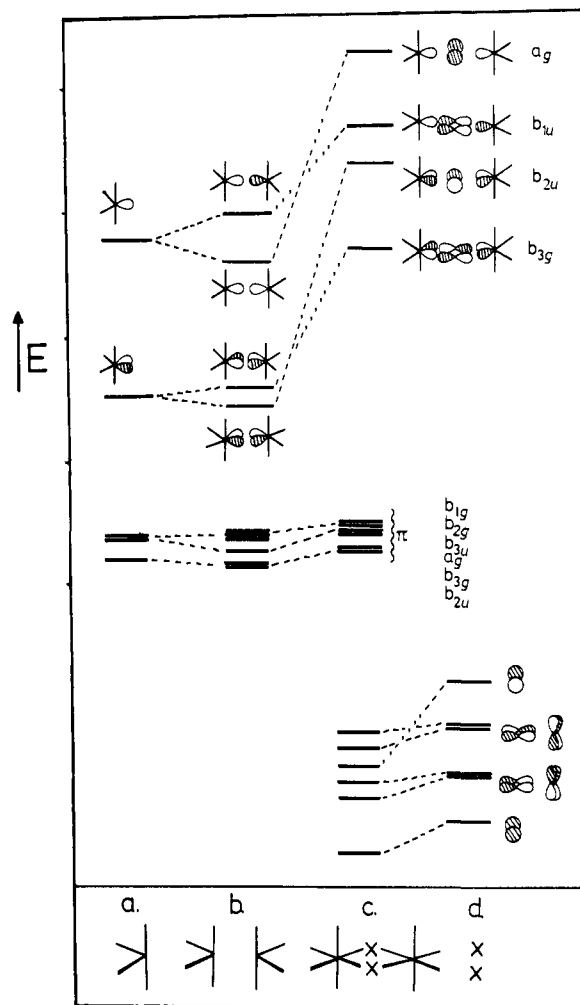
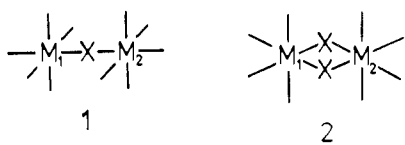
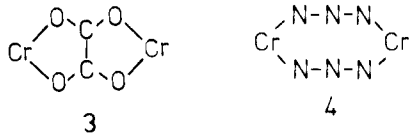


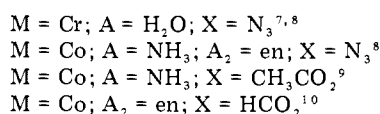
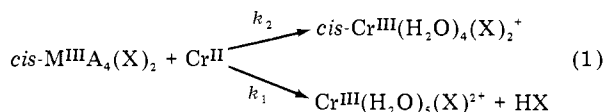
**Figure 1.** Assembly of the molecular orbital diagram for a symmetrically doubly bridged species  $M_2X_{10}$  (c) from those of two octahedral cis divacant units (a) and a bridging  $X_2$  group (d) via the  $M_2X_8$  unit (b). The diagram is only semiquantitative. The metal d orbital region and that of the bridging  $X_2$  group are drawn to different scales.



in redox reactions is less forthcoming than that for single bridging but it has been unequivocally established in several cases. The isotopic exchange between  $*Cr^{2+}$  and  $Cr(H_2O)_4C_2O_4^+$  and the aquation<sup>6</sup> (catalyzed by  $Cr^{II}$ ) of  $cis-Cr(H_2O)_2(C_2O_4)_2^-$  probably occur via the doubly bridged chelated arrangement **3** and isotopic exchange between



$Cr(H_2O)_4(N_3)_2^+$  and  $*Cr^{2+}$  also shows<sup>7</sup> transfer of two coordinated ligands during redoxidation. This confirms the presence of either a short-lived intermediate or a transition state perhaps of the structure **4** (or an alternative arrangement where a single nitrogen atom of each azide is coordinated to both chromium atoms). Reaction via the inner-sphere route involving transfer of a single azide ligand occurs 30 times slower.<sup>8</sup> Similar two-ligand and one-ligand pathways (as we shall see later, these are not necessarily associated with double-



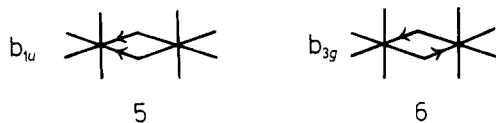
and single-bridged complexes) occur in other systems (eq 1). In addition to this direct evidence for double bridging there is less conclusive evidence<sup>11</sup> concerning the dependence of the rate on hydrogen ion concentration in situations where hydroxide ion may be transferred. In addition to doubly bridged species postulated to occur as intermediates or transition states in these redox reactions, many examples are known as stable species in crystals amenable to X-ray characterization.

### Molecular Orbital Structure of Doubly Bridged Species

Figure 1 shows the synthesis of a molecular orbital diagram for a symmetrically bridged species  $M_2X_{10}$  from those of an "octahedral cis-divacant"  $MX_4$  fragment and an  $X_2$  unit. While most of our arguments will be symmetry and overlap based, we have supported these ideas with quantitative molecular orbital calculations of the extended Hückel sort on the model species  $Cr_2Cl_{10}^{2+}$ . The details are given in the Appendix. Calculations of this type, however, mimic well the relative energy changes of transition-metal systems associated with angular deformations but perform less satisfactorily when the distortion coordinate involves changes in internuclear distances between bonded atoms. The numerical results of our calculations will be used with caution.

Each  $MX_4$  unit provides two frontier orbitals which point toward the vacant sites of the octahedron.<sup>12</sup> Bonding and antibonding partners arise when the two  $MX_4$  units are brought together (Figure 1b). These orbitals are further displaced in energy when (antibonding) interactions with the bridging  $X_2$  unit are switched on (Figure 1c). Since all the bridging X-X bonding and antibonding orbitals are occupied there is to first order a nonbonded situation between these atoms. (This is not the case for the oxalate bridge of **3** where the carbon atoms are joined together.) The predominantly metal d orbitals are of two energetic types. The deeper lying orbitals are  $\pi$  bonding with respect to the coordinated ligands (we will refer to these orbitals as a block) and the higher lying orbitals, whose energy varies significantly with geometry, involved in metal-ligand  $\sigma$  interactions.

Whereas the singly bridged species  $M_2X_{11}$  could distort asymmetrically in only one basic way,<sup>1</sup> there are two routes open to the doubly bridged  $M_2X_{10}$  system (**5, 6**) leading to very



different products as the fragments separate. Figure 2 shows how the molecular orbitals of the symmetrically bridged unit change in energy on distortion. There are much smaller energy changes associated with the  $\pi$  orbitals (not shown). The directions of the orbital energy changes are readily understood since the orbitals of the symmetric species will correlate with the orbitals of the four-, five-, and six-coordinate mononuclear species. The energies of the octahedrally based mononuclear species are given in Figure 3 in terms of the parameters of the angular overlap method.<sup>13</sup> Perturbation theory arguments also assist in tracing the direction of the orbital energy changes. For example, the  $b_{3g}$  and  $b_{2u}$  orbitals of different symmetry at the symmetric geometry become of the same symmetry species ( $b_1$ ) on a  $b_{1u}$  distortion. They mix together and "repel" each

Table I. Representative Structures of  $M_2X_{10}$  Species

electronic configuration	molecule	bridge atoms	bond lengths				distortion mode	ref
			1	2	3	4		
$d^0d^0, \pi^0$	$Ti_2^{IV}Cl_{10}^{2-}$	Cl	2.481	2.506	<i>a</i>		small, $b_{3g}$	14
$d^1d^1, \pi^2$	$Mo_2^{VI}S_2O_2(L\text{-histidinato})_2$	S	2.32	2.30	2.34	2.31	small, $b_{3g}$	15
$hsd^3hsd^3, \pi^6$	$Cr^{III}(OH)_2phen_4^{4+}$	O	1.931	1.927	1.931	1.937	small, $b_{3g}$	16
$lsd^5lsd^5, \pi^{10}$	$Re_2^{II}Cl_2(dppe)_2^{2+}$	Cl	2.503	2.496	<i>a</i>		small, $b_{3g}$	17
$lsd^6lsd^6, \pi^{12}$	$Ru_2^{II}(C_2O_4)(terpy)_2^b$	O	2.113	2.096	<i>a</i>		small, $b_{3g}$	18
$lsd^6lsd^6, \pi^{12}$	$Co_2^{II}(SR)_2(S_2CSR)_4$	S	2.250	2.242	<i>a</i>		small, $b_{3g}$	19
$hsd^4hsd^3, \pi^6 b_{3g}^1$	$Mn_2^{III,IV}O_2(bpy)_4^+$	O	1.784	1.784	1.856	1.853	large, $b_{1u}$	20
$lsd^7lsd^7, \pi^{12} b_{3g}^1 b_{2u}^1$	$Co_2^{II}(L_2)L_8^c$	O	2.125	2.158	<i>a</i>		small, $b_{3g}$	21
$lsd^6lsd^8, \pi^{12} b_{3g}^2$	$Mn(NO_2)Cp(NO)_2MnCpNO$	N	1.775	1.775	1.943	1.943	large, $b_{1u}$	22
$lsd^6lsd^8, \pi^{12} b_{3g}^2$	$Pt_3Cl_{12}^{2- d,e}$	Cl	2.300	2.300	2.384	2.384	<sup>e</sup> small, $b_{1u}$	23
$hsd^8hsd^8, \pi^{12} b_{3g}^1 b_{2u}^1 b_{1u}^1 a_g^1$	$Ni_2^{II}(N_3)_2Am_2^{2+ f}$	N	2.195	2.069	<i>a</i>		small, $b_{3g}$	24
$lsd^9lsd^9, \pi^{12} b_{3g}^2 b_{2u}^2 b_{1u}^1 a_g^1$	$Cu_2^{II}(pyNO)_4Cl_4^d$	O	1.977	2.039	<i>a</i>		small, $b_{3g}$	25
$d^{10}d^{10}, \pi^{12} b_{3g}^2 b_{2u}^2 b_{1u}^2 a_g^2$	$Cu_2^I(S=C(NH_2)_2)_6^{2+ d}$	S	2.367	2.429	<i>a</i>		small, $b_{3g}$	26

<sup>a</sup> Centrosymmetric unit. <sup>b</sup> Chelate. <sup>c</sup> L = 2(1*H*)-tetrahydropyrimidone. <sup>d</sup> Based on square-planar coordination. <sup>e</sup> Pt<sup>IV</sup>-Pt<sup>III</sup>-Pt<sup>IV</sup> unit. <sup>f</sup> Am = 2,2',2''-triaminotriethylamine.

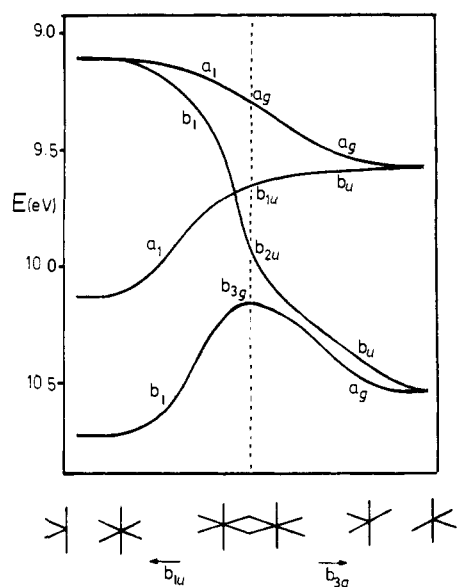


Figure 2. Behavior of d orbital energy levels involved primarily in  $\sigma$  interactions on distortion of the symmetrical bridged species  $M_2Cl_{10}$ . At the extremity of the  $b_{1u}$  distortion the lowest two levels are those of the octahedral cis-divacant unit and the degenerate upper pair of the  $e_g$  levels of the octahedron. At the extremity of the  $b_{3g}$  distortion there are two pairs of levels each corresponding to one of the levels of the square pyramid.

other in energy as the distortion proceeds. The stability pattern of the symmetrically doubly bridged species as a function of detailed electronic configuration mirrors that of the singly bridged molecule described in our previous study.<sup>1</sup> For most electronic configurations it is predicted to be stable but for the same few configurations that the symmetrically singly bridged species was calculated to be unstable we find that the analogous doubly bridged molecule should distort away from the symmetric geometry. We use a notation similar to that used before to describe the electronic configuration of the species in terms of the d orbital configurations of the two separated reactants and that of the complex. The actual numerical results of the calculations depend upon the exact form of the molecular motions of **5** and **6**, whether we choose to keep the metal-metal distance constant, for example, on asymmetrization. However, the trends as a function of d electron configuration are independent of the model selected. For the  $d^0d^0, \pi^0$  molecule we calculate that the symmetrically bridged species is most stable but that the energy cost of asymmetrization is not large. Specifically the  $b_{3g}$  distortion is always found to be of lower energy. When considering the energetics of other d orbital configura-

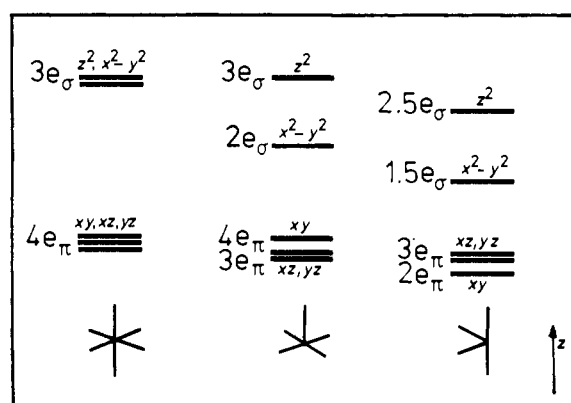
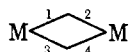


Figure 3. Angular overlap d orbital energies of six-, five-, and four-coordinate complexes.

rations via Figure 2 we will need to bear this result in mind. This  $d^0d^0, \pi^0$  result holds for all configurations  $d^m d^n, \pi^{n+m}$  since the energy changes of the  $\pi$  block generally favor the symmetric geometry. Figure 2, however, shows that occupation of the  $\sigma b_{3g}$  orbital will strongly encourage asymmetrization and furthermore the most favored route is the one of species  $b_{1u}$ . We could view this perhaps as a second-order Jahn-Teller distortion. Thus configurations  $b_{3g}^1, b_{3g}^2$ , and  $b_{3g}^2 b_{2u}^1$  are unstable in this way. On symmetrical occupation of  $b_{3g}$  and  $b_{2u}$  orbitals the diagram indicates that the  $b_{3g}$  distortion is of lower energy than the corresponding  $b_{1u}$  motion ( $b_{3g}^1 b_{2u}^1$  and  $b_{3g}^2 b_{2u}^2$  configurations). For other electronic configurations the symmetric geometry is predicted but with a low-energy  $b_{3g}$  distortion. These results are borne out well when crystal structures of these doubly bridged systems are surveyed (Table I). Species without asymmetric occupation of  $b_{3g}$  and  $b_{2u}$  orbitals show approximately symmetric bridges with small  $b_{3g}$  distortions. Many of these examples are centrosymmetric. We also include three examples based on square-planar coordination. There are no genuine  $lsd^8$  octahedral species to test out the prediction for the  $lsd^8 lsd^8$  system and  $d^9 MY_6$  octahedra usually have very long axial bonds making formal distinction between four and six coordination difficult. Our  $Cu^{II}$  representative, for example, contains square-planar units with two extra, weakly coordinated ligands. However, both octahedral  $hsd^3hsd^4$  and  $lsd^6lsd^8$  examples are strongly distorted, and, as predicted, along the  $b_{1u}$  coordinate (**7, 8**). The second example **8** is a rather complex one. Firstly, each metal atom is chemically different (coordinated NO and NO<sub>2</sub>), and secondly, when considering systems with nitrosyl ligands we need to use the

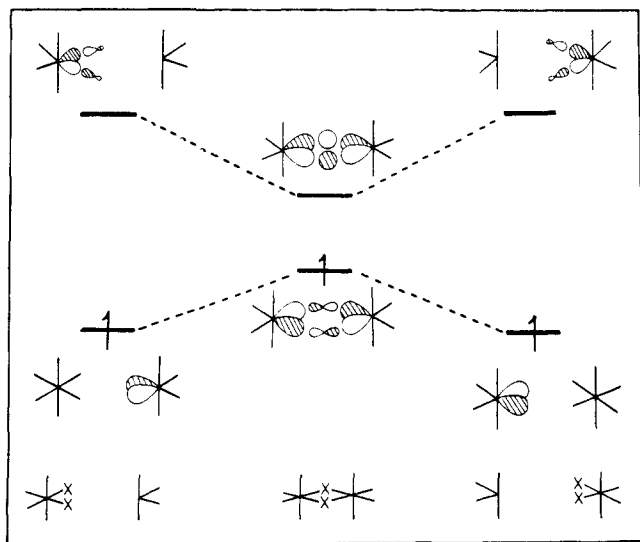
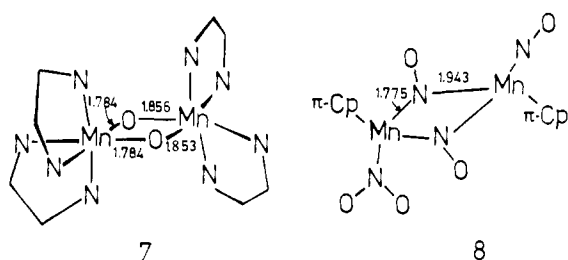
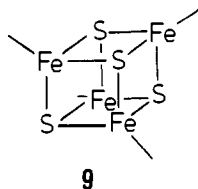


Figure 4. The intimate process of electron transfer via the doubly bridged structure for, e.g., the  $\text{Cr}^{\text{II}}/\text{Cr}^{\text{III}}$  system.



$\{\text{MNO}\}^n$  notation of Enemark and Feltham<sup>27</sup> rather than the usual  $d^n$  description. The two centers in this case are  $\{\text{MNO}\}^6$  and  $\{\text{MNO}\}^8$  which, since the MNO group is linear, we regard as being equivalent to  $d^6$  and  $d^8$  configurations. Thirdly, we regard  $\pi\text{-Cp}$  as occupying three (fac) coordination sites. We found<sup>1</sup> a violation of our simple scheme for the singly bridged diamagnetic  $\text{Co}^{\text{II}}$  complex  $\text{Co}_2\text{I}_3(\text{CNPh})_8^+$  in our previous study. The small  $b_{3g}$  distortion of the  $\text{Co}^{\text{II}}$  complex of Table I, however, is in accord with our predictions, since it is a paramagnetic species<sup>29</sup> and therefore probably has the  $b_{3g}^1 b_{2u}^1$  configuration.

Asymmetric double bridges are found in other species. In  $\text{Fe}_4\text{S}_4$  cubane-type structures<sup>30</sup> 9, models for the active site in



4-Fe and 8-Fe proteins which contain tetrahedrally coordinated iron, the symmetry is usually reduced to  $D_{2d}$  via bridge asymmetrization. This distortion has been ascribed<sup>31</sup> to the presence of an orbitally degenerate electronic state and the consequences of the Jahn-Teller theorem.

#### Application to Redox Reactions

Our theoretical considerations and the available crystallographic results lead us to predict that for systems with an asymmetric occupation of  $b_{3g}$  and  $b_{2u}$  orbitals the symmetrically bridged geometry corresponds to a transition state with the path of steepest descent associated with the  $b_{1u}$  distortion. For all other electron configurations, the symmetric geometry may be an intermediate with the lowest energy decay pathway probably associated with the  $b_{3g}$  route. All of the well-char-

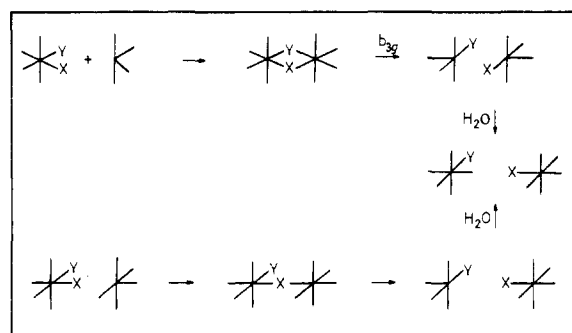
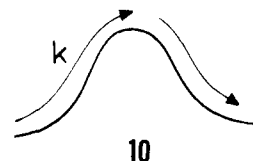


Figure 5. One-ligand transfer during a redoxidation via the doubly bridged (top) and singly bridged (bottom) routes.

acterized redox processes involving two-ligand transfer have involved  $\text{Cr}^{\text{II}}/\text{Cr}^{\text{III}}$  ( $\text{hsd}^4\text{hsd}^3$ ) or  $\text{Cr}^{\text{II}}/\text{Co}^{\text{III}}$  ( $\text{hsd}^4\text{lsd}^6$ ) systems (eq 1). These two species have electronic configurations  $\pi^n b_{3g}^1$  such that the symmetrically doubly bridged structure is predicted to decay via the  $b_{1u}$  motion and give rise to two ligand transfer. The lack of direct observation of the doubly bridged species is in accord with our prediction that it corresponds to a transition state. Interestingly  $\text{lsd}^6\text{lsd}^6\pi^{12}\text{Co}_2^{\text{III}}(\mu\text{-SR})_2(\text{S}_2\text{CSR})_4$ , stable as an approximately symmetrically bridged species, undergoes an irreversible two-electron reduction.<sup>31</sup> This may be understood if the reduced product dissociates immediately to monomers. Similarly  $\text{Co}_2^{\text{III}}(\mu\text{-OH})(\mu\text{-C}_2\text{O}_4)(\text{triammine})_2$  decays to monomeric  $\text{Co}^{\text{II}}$  species on reduction.<sup>33</sup> Population of the  $b_{3g}$  orbital is thus associated with instability of the bridged molecule.

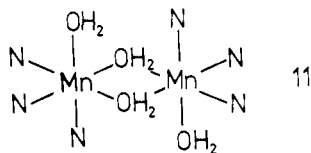
How the electron is "transferred" via this doubly bridged transition state is very similar to the scheme devised for the singly bridged route<sup>1,34</sup> and is shown in Figure 4. Using our previous terminology this is a smooth type I electron transfer over an energy barrier 10 (whose origin is readily appreciated



from Figure 4) where the reaction coordinate involves the  $b_{1u}$  motion of the bridging atoms. Similar profiles are expected for all electron transfers where the electron configuration of the symmetrically bridged species is either  $b_{3g}^1$ ,  $b_{3g}^2$  or  $b_{3g}^2 b_{2u}^1$ . An interesting observation<sup>35</sup> is that in all the double-bridging instances studied to date at least one of the partners has a delocalized  $\pi$  bond system. It is, however, difficult to evaluate those structural factors which will favor  $k_2$  compared to  $k_1$  (1). In general there have been no systematic studies of the rate of the two-ligand pathway as a function of the nature of the ligands attached to the metal. We would expect similar dependence upon the nature of the bridging and nonbridging ligands as determined<sup>1</sup> in the singly bridged case.

The extension of similar reasoning to other electronic configurations, e.g.,  $d^n d^m$ ,  $\pi^{n+m}$  and  $\text{hsd}^8\text{hsd}^8$  systems, leads to the perplexing problem shown in Figure 5. Here the symmetrically double bridge is predicted to be stable but decay is probably via the  $b_{3g}$  motion leading to two five-coordinate units. Experimental observation of one-ligand transfer by product analysis, however, will not distinguish between double- or single-bridged intermediates or a mechanism involving both pathways (Figure 5). We have no reliable quantum-mechanical method at present to predict which route would be preferred. In many cases the doubly bridged route will be insignificant since the process initially involves loss of two solvent molecules from the coordination sphere of the reductant. Many redox studies, however, have used the very labile species  $\text{Cr}^{\text{II}}$

as reductant, where this objection does not apply. This doubly bridged one-ligand transfer route may be more prevalent than imagined. There is crystallographic evidence for doubly bridging water molecules (the solvent in which the majority of these reactions are studied) in the  $\text{Mn}_2\text{N}_6(\text{H}_2\text{O})_4$  unit (**11**)



found<sup>36</sup> in the polymeric species  $\text{Mn}_2^{\text{II}}\text{Ru}^{\text{II}}(\text{CN})_6(\text{H}_2\text{O})_4 \cdot 4\text{H}_2\text{O}$ . Spectral examination of the solution intermediate in these cases has usually focused on oxidation-state identification rather than detailed characterization (difficult) of the species itself. Doubly bridged intermediates which decay by the  $b_{3g}$  route are possible for processes involving both smooth (for example,  $t_{2g} \rightarrow t_{2g}$  transfer in the  $\text{Fe}^{\text{II}}/\text{Fe}^{\text{III}}$  system) and sudden (for example,  $e_g \rightarrow t_{2g}$  transfer in the  $\text{Cr}^{\text{II}}/\text{Ru}^{\text{III}}$  system) electron transfer. Just how important the  $b_{3g}$  decay of the doubly bridged intermediate leading overall to one-ligand transfer (i.e., the relative rates of the two processes of Figure 5) is an important experimental question which needs to be answered.

**Acknowledgment.** I acknowledge useful conversations with Mr. G. Beekman and Professor J. H. Espenson.

### Appendix

The Slater exponents and ionization potentials used in the EHMO<sup>37</sup> calculations follow: Cr, 3d 2.500, -11.50; 4s 1.700, -9.00; 4p 1.700, -5.00. Cl, 3s 2.033, -30.00; 3p 2.033, -15.00. In the symmetrical bridge the Cr-Cl distances were 2.28 (terminal) and 2.54 Å (bridging). On asymmetrization the bridging distances were gradually made equal to the terminal ones. Calculations were also performed with Cr-Cl (terminal) = 2.24 and 2.32 Å (with proportionately different values for Cr-Cl (bridging)) without any qualitative differences. Moving the two fragments apart during the asymmetrization process made the symmetric, undistorted structure less stable relative to the distorted geometries.

### References and Notes

- (1) J. K. Burdett, *Inorg. Chem.*, **17**, 2537 (1978).
- (2) For a selection of pertinent references concerning transition-metal redox reactions see ref 1.
- (3) R. D. Cannon in "Inorganic Reaction Mechanisms", Vol. 5, A. McAuley, Ed., Specialist Periodic Reports, The Chemical Society, London, 1977.
- (4) D. E. Pennington "Coordination Chemistry", *ACS Monogr.*, No. 174 (1978).
- (5) C. Hwang and A. Haim, *Inorg. Chem.*, **9**, 500 (1970).
- (6) T. Spinner and G. M. Harris, *Inorg. Chem.*, **11**, 1067 (1972).
- (7) R. Snellgrove and E. L. King, *J. Am. Chem. Soc.*, **84**, 4609 (1962).
- (8) A. Haim, *J. Am. Chem. Soc.*, **88**, 2324 (1966).
- (9) R. T. M. Fraser, *J. Am. Chem. Soc.*, **85**, 1747 (1963).
- (10) J. R. Ward and A. Haim, *J. Am. Chem. Soc.*, **92**, 475 (1970).
- (11) H. Diaz and H. Taube, *Inorg. Chem.*, **9**, 1304 (1970).
- (12) The frontier orbitals are similar to those of  $\text{M}(\text{CO})_4$  described in M. Elian and R. Hoffmann, *Inorg. Chem.*, **14**, 1058 (1975).
- (13) J. K. Burdett, *Adv. Inorg. Chem. Radiochem.*, **21**, 113 (1978).
- (14) T. J. Kristenmacher and G. D. Stucky, *Inorg. Chem.*, **10**, 122 (1971).
- (15) B. Spivack, A. P. Gaughan, and Z. Dori, *J. Am. Chem. Soc.*, **93**, 5265 (1971).
- (16) J. T. Veal, W. E. Hatfield, and D. J. Hodgson, *Acta Crystallogr., Sect. B* **29**, 12 (1973).
- (17) J. A. Jaecker, W. R. Robinson, and R. A. Walton, *J. Chem. Soc., Chem. Commun.*, 306 (1974).
- (18) P-T Cheng, B. R. Loescher, and S. C. Nyburg, *Inorg. Chem.*, **10**, 1275 (1971).
- (19) D. F. Lewis, S. J. Lippard, and J. A. Zubieta, *J. Am. Chem. Soc.*, **94**, 1563 (1972).
- (20) P. M. Plaskin, R. C. Stoufer, M. Mathew, and G. J. Palenik, *J. Am. Chem. Soc.*, **94**, 2121 (1972).
- (21) M. E. Brown, J. N. Brown, and L. M. Trefonas, *Inorg. Chem.*, **11**, 1836 (1972).
- (22) J. L. Calderon, F. A. Cotton, B. G. DeBoer, and N. Martinez, *J. Chem. Soc., Chem. Commun.*, 1476 (1974).
- (23) P. M. Cook, L. F. Dahl, and D. W. Dickerhoof, *J. Am. Chem. Soc.*, **94**, 5511 (1972).
- (24) C. G. Pierpont, D. N. Hendrickson, D. M. Duggan, F. Wagner, and E. K. Barefield, *Inorg. Chem.*, **14**, 604 (1975).
- (25) J. C. Morrow, *J. Cryst. Mol. Struct.*, **4**, 243 (1974).
- (26) M. S. Weininger, I. F. Taylor, and E. L. Amma, *Inorg. Chem.*, **13**, 2835 (1974).
- (27) J. H. Enemark and R. D. Feltham, *Coord. Chem. Rev.*, **13**, 339 (1974).
- (28) D. Baumann, H. Endres, H. J. Keller, and J. Weiss, *J. Chem. Soc., Chem. Commun.*, 853 (1973).
- (29) A. G. Pierce, Jr., U.S. Department of Agriculture, private communication.
- (30) L. Que, M. A. Bobrik, J. A. Ibers, and R. H. Holm, *J. Am. Chem. Soc.*, **96**, 4168 (1974).
- (31) C. Y. Yang, K. H. Johnson, R. H. Holm, and J. G. Norman, *J. Am. Chem. Soc.*, **97**, 6596 (1975).
- (32) D. Coucouvanis, S. J. Lippard, and J. A. Zubieta, *J. Am. Chem. Soc.*, **92**, 3342 (1970).
- (33) I. Baldea, K. Weighardt, and A. G. Sykes, *J. Chem. Soc., Dalton Trans.*, 78 (1977).
- (34) L. E. Orgel, Report 10<sup>eme</sup> Conseil Chimique, Solvay, Bruxelles, 1956.
- (35) H. Taube, "Electron Transfer Reactions of Complex Ions in Solution", Academic Press, New York, 1970, p 69.
- (36) M. Ruegg, A. Ludi, and K. Rieder, *Inorg. Chem.*, **10**, 1773 (1971).
- (37) R. Hoffmann, *J. Chem. Phys.*, **39**, 1397 (1963); R. Hoffmann and W. N. Lipscomb, *ibid.*, **36**, 2179, 3489 (1962).